



DESY SUMMER STUDENT PROGRAMME

Coherent X-ray Diffractive Imaging

Reconstruction of simulated scattering data

Simone De Camillis

University of Pisa, Italy

19th July - 8th September

Supervisors:

Ivan Vartanyants

Oleksandr Yefanov

Abstract

The coherent X-ray diffractive imaging (CXDI) is a good method to investigate the structure of matter. It's possible to reconstruct the electron density of a sample from its diffraction patterns using a phase retrieval algorithm.

Simulated 3D scattering data of several colloidal samples, with different beamstop size, are reconstructed. The reconstruction method using program *recon* and its main properties is shown.

Contents

1	Introduction	3
2	Phase retrieval algorithm	3
2.1	Error-Reduction and Hibrid Input-Output algorithms	4
3	Coherent X-ray scattering simulation	5
4	Reconstruction of a sample	6
4.1	Spherical object	6
4.2	Spherical object with beamstop and statistical noise	7
4.3	Ellipsoidal object with small beamstop	10
4.4	Ellipsoidal object with bigger beamstop and loose support	13
5	Conclusion	15
6	Acknowledgments	15

1 Introduction

The coherent X-ray diffractive imaging (CXDI) is an important techniques to relieve the structure of a sample. It consists to illuminate a finite sized object with a coherent X-ray, record the scattered radiation in the far-field limit and invert the signal in order to reach informations about the sample: the diffraction pattern is closely connected with the Fourier transform of the sample's electron density [1]:

$$I(R, \theta, \phi) \propto \left| \int n_{el}(\mathbf{r}) e^{i(\mathbf{k}' - \mathbf{k}) \cdot \mathbf{r}} d\mathbf{r} \right|^2 \cdot \left(\frac{d\sigma}{d\Omega} \right) \quad (1)$$

By rotating the sample along the z-axis, its 3D reciprocal space amplitude can be acquired.

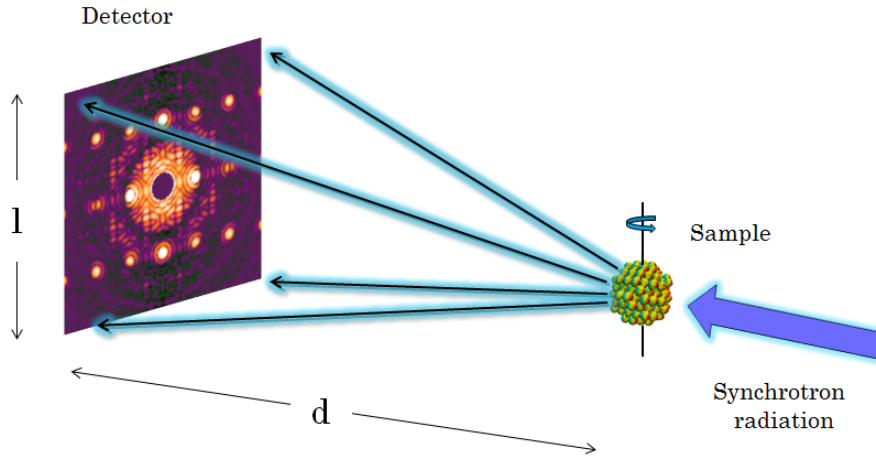


Figure 1: Experiment Diagram.

It's not trivial to invert Eq. (1) because of the phase problem. The experimental data gives only the amplitude of the signal without the phase, but we need both of them to reconstruct the object.

If a diffraction pattern could be sampled at twice of the Nyquist frequency, in other words oversampled, it would be possible to retrieve all the necessary information [1].

2 Phase retrieval algorithm

There is a computer algorithm that incorporates the oversampling as real-space constraints. A good description and comparison of several numerical implementations of the phase retrieval algorithm are shown by Fienup [2].

To understand the process, we show here the Input-Output (IO) algorithm. It operates by successively Fourier transforms of the data between the real and reciprocal space,

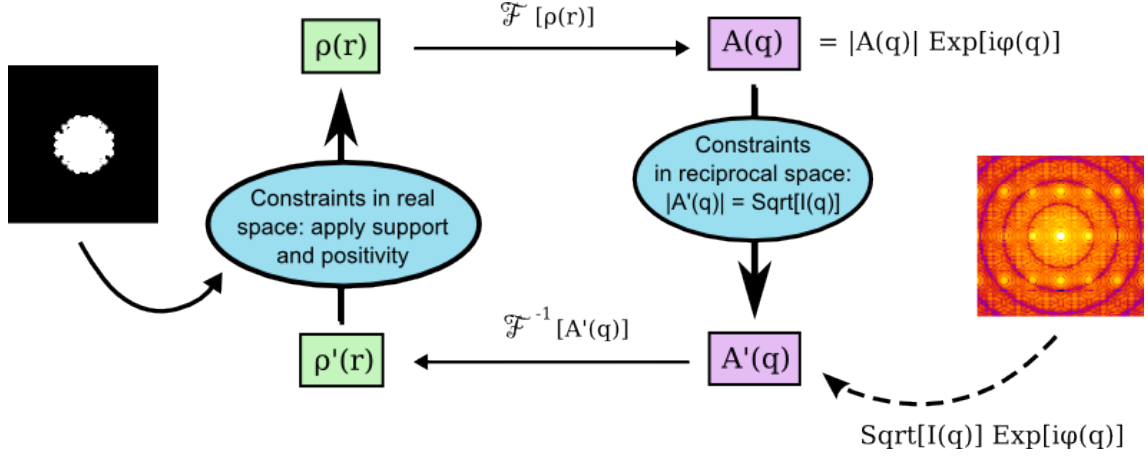


Figure 2: Diagram of Input Output algorithm.

applying constraints in both of them. We have the final result when constraints doesn't change the data. In Fig. 2 a representation of the IO algorithm is shown.

For start a guess of the electron density distribution $\rho(r)$ is necessary. It's obtained performing an inverse Fourier transform of the square root of the measured intensities, multiplied by a random phase factor ψ : $\sqrt{I(q)} \cdot \exp[i\psi(q)]$.

The first step is to calculate the new complex scattering amplitude $A(q) = |A(q)| \cdot \exp[i\phi(q)]$ with a Fourier transform. But we want that our object respects the reciprocal space constraint, that is, the modulus of the complex scattering amplitude $A(q)$ must be equal to $\sqrt{I(q)}$. Hence we impose this condition to our data.

In the next step we calculate the new estimate of electron density $\rho'(r)$ performing a inverse Fourier transform. Finally real space constraints are applied to our estimated object: the (optional) request that $\rho'(r)$ is positive and the application of a sort of mask, the support, which sets $\rho'(r)$ to be the same value in the support region and reduced it otherwise. In particular the last operation gives the following result:

$$\rho_{k+1}(r) := \begin{cases} \rho_k(r), & \text{in the support,} \\ \rho_k(r) - \beta \rho'_k(r), & \text{outside the support,} \end{cases} \quad (2)$$

where β parameter quantifies the reduction percentage.

The application of the real and Fourier constraints allows to improve the phase factor in each iteration.

2.1 Error-Reduction and Hibrid Input-Output algorithms

In this work Error-Reduction (ER) and Hibrid Input-Output (HIO) algorithms are used. They have the same basic idea of IO algorithm. The differences are in the way to apply the support.

In HIO algorithm we have to consider $\rho_k(r)$ and $\rho'_k(r)$ electron density distributions at the k -th iteration. The new density estimate is a combination of the old ones, such that

$$\rho_{k+1}(r) := \begin{cases} \rho'_k(r), & \text{in the support,} \\ \rho_k(r) - \beta\rho'_k(r), & \text{outside the support.} \end{cases} \quad (3)$$

The idea of the ER algorithm is easier: we leave the same distribution in the support region and we set null value otherwise.

$$\rho_{k+1}(r) := \begin{cases} \rho'_k(r), & \text{in the support,} \\ 0, & \text{outside the support.} \end{cases} \quad (4)$$

3 Coherent X-ray scattering simulation

In this work we don't analyse real diffractive patterns but we use simulated ones. The programme *Moltrans* provides simulated scattering data.

The main parameters for a simulated experiment are the sample (the distribution of particles inside the sample as a .pdb file), the wavelength of the light, the sample-detector distance (d) and the detector size (l). *Moltrans* receives other optional informations that we omit here.

With these three variables the image resolution is determinated. In fact, from the diffractive law, we can calculate the smallest distance Δx between two consecutive interference fringes, that is, the smallest distinguishable distance.

$$\lambda = 2\Delta x \sin \theta \quad (5)$$

The angle range is limited by the experiment geometry. As it's shown in Fig. 3, the bigger angle is related with the lengths d and l by trigonometrical equation. Combining

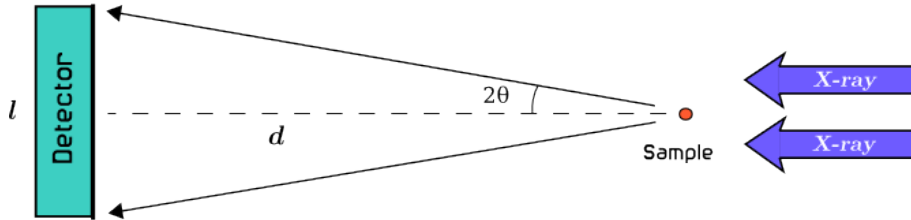


Figure 3: Experiment layout.

these two relations, we can obtain the resolution:

$$\Delta x = \frac{\lambda}{2 \sin \left[\frac{1}{2} \arctan \left(\frac{l}{2d} \right) \right]}. \quad (6)$$

We have to choose also the size of the image (in pixels) and the number of sample rotations along its axis. The latter should be such that scattering informations can

cover all the 3D q-space pixels: for this reason we select a rotation of 180 degrees and search the number of scattering acquisitions such that in a singular rotation the plane doesn't overcome pixel length.

4 Reconstruction of a sample

The support shape plays an important role in the reconstruction process. As we can see in the IO algorithm, results are strongly determined by the choice of the support. But at the beginning we don't know its real shape. Therefore the shape search is performed during the reconstruction process.

The programme used for the reconstruction is *recon*. It has to receive some informations about the size of the image (*SizRec*), the size of the support (*SizSup*, one parameter for a spherical shape, 2 or 3 for a rectangular shape) or directly a support file, the (optional) request of object positivity and instructions about the reconstructive iterations.

An example of the configuration list is the following:

```
SizRec: 135 135 135
SizSup: 55
Positiv: 0
[.]

hio    100 1 0.8 0
er     50 1 0.8 0
ShrinkWrap    1 10 0
[...]
hio    100 1 0.8 0
er     50 1 0.8 0
```

In *hio* and *er* instructions, the first and the third parameters are respectively the number of iterations and the β constant. Function *ShrinkWrap* allows to change original support cutting out the points near support with values of $\rho'(r)$ below a determined threshold: in this case, the area with less 10% of the maximum intensity is removed.

A appropriate choice of instructions and parameters allows to obtain a good final image.

4.1 Spherical object

The first object that we'll reconstruct is a spherical bubble cluster with diameter of about 1610 nm, shown in Fig. 4(a). 720 scattering amplitudes were acquired rotating the sample of 180 degrees.

For this simulation we used a wavelength $\lambda = 1.57 \text{ \AA}$, sample-detector distance $d = 5000$ mm and the detector size $l = 52$ mm. According with Eq. 3, the resolution for this experimental configuration is about $\Delta x = 30$ nm.

The Fig. 4(b) is the simulated scattering pattern given by *Moltrans*. In this case the reconstruction is easy because it's an ideal data without any missing informations. The

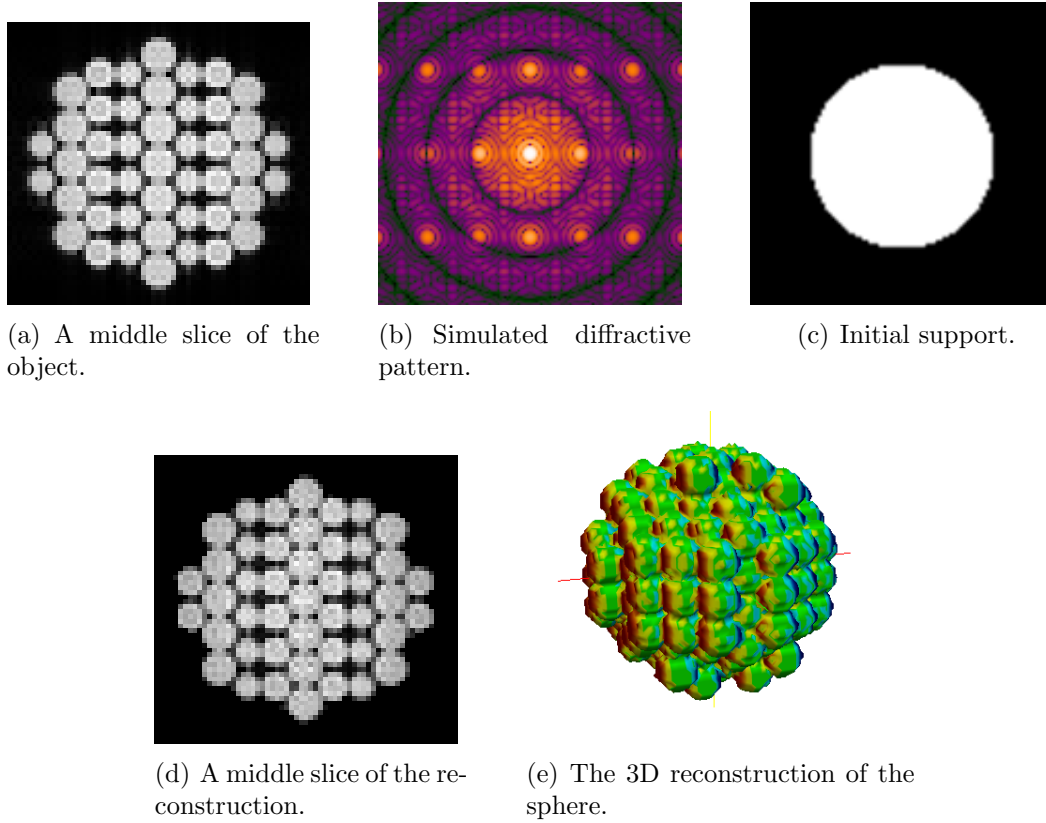


Figure 4: Simulated scattering and reconstruction of the spherical sample.

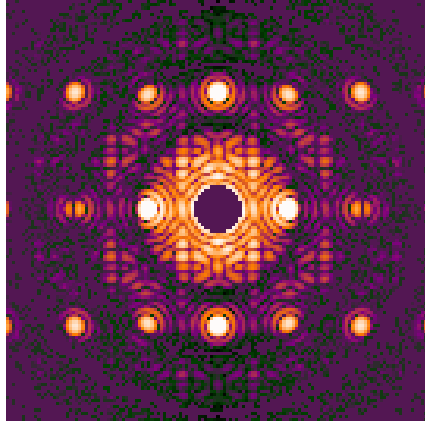
first step is finding a right support. The size estimate can be found from fringes in the diffraction pattern. It's enough running two times the cycle of instructions above to find a good shape. Iterating again four times the same cycle with the new support, we achieve a good result: in Fig. 4(d) is shown one slice of the reconstructed 3D image. The programme *Paraview* shows iso-surface of the reconstruction 3D object (Fig. 4(e)).

4.2 Spherical object with beamstop and statistical noise

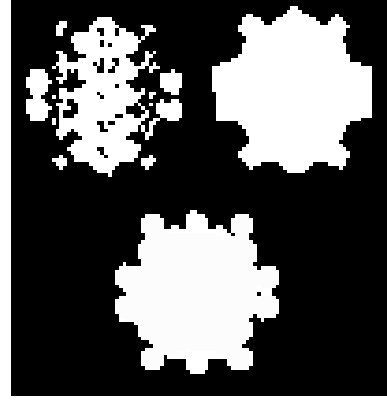
In the actual experiment there is less information: the presence of a beamstop in front of the detector, in order to avoid damages, and the statistical noise in the experimental data. Now we want also simulate these problems in our pattern, as you can see in Figure 5(a).

In order to find the support, we have to run several cycles of the following instructions. For scattering data with noise, it's better to start with the option *Positive 1*.

```
SizRec: 135 135 135
SizSup: 55
Positiv: 1
```



(a) Simulated diffractive pattern.



(b) Improving of the support shape.

Figure 5: Simulated scattering and reconstruction of the spherical sample with beamstop and statistical noise.

```
hio    80 1 0.9 0
er     60 1 0.8 0
ShrinkWrap    1 10 0
```

To improve the shape, we can repeat this step more times, making manual adjustments (for example, to get more smooth the profile and to fill internal holes: Fig. 5(b)) Obtained a goos support, the reconstruction is possible using the parameter *Positive 0* and one cycle of *hio* and *er* with the same iteration numbers. The result (Fig. 6(a)) is not very good: the center of the object is confused and not sharp.

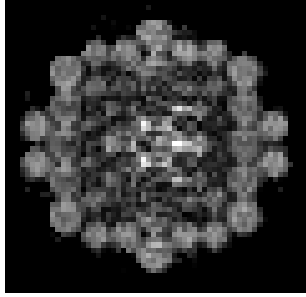
The missing information in the center (where is the beamstop) and at corners of the 3D reciprocal space gives problems to the reconstruction. For these reason, the function *FixFreeEvolve* fills the missing intensities in the diffraction pattern with rescaled Fourier transform of the support. It's possible to replace the intensity within a circle, specified by first parameter, and optionally besides a second one (the second parameter). Using the last support, we get reconstruction running three times the following cycle:

```
Positiv: 0
```

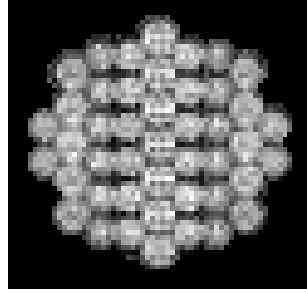
```
FixFreeEvolve 17
hio    100 1 0.9 0
er     50 1 0.8 0
```

Now the result is also well-defined in the middle (see Fig. 6(b)).

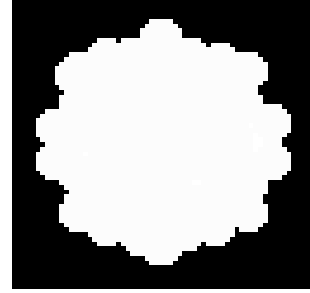
We can also compare the reconstructed reciprocal space in Fig. 6(d) with the scattering amplitude without beamstop, Fig. 4(b).



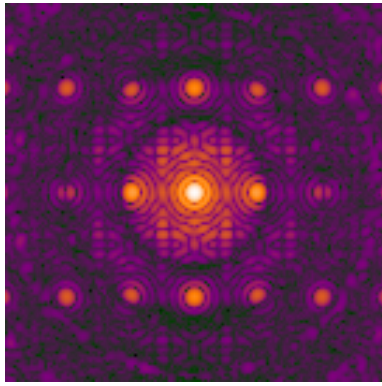
(a) The reconstruction.



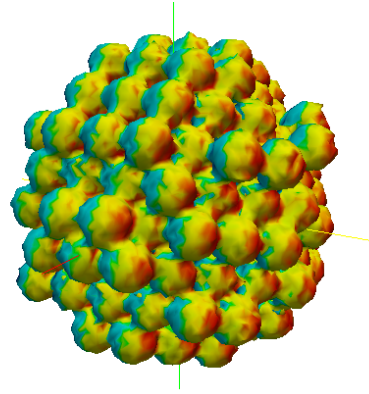
(b) The reconstruction using FixFreeEvolve.



(c) The final support of the reconstruction.



(d) The reconstructed reciprocal space with FixFreeEvolve.

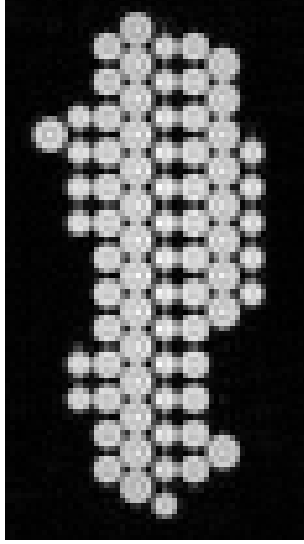


(e) The iso-surface of the 3D object.

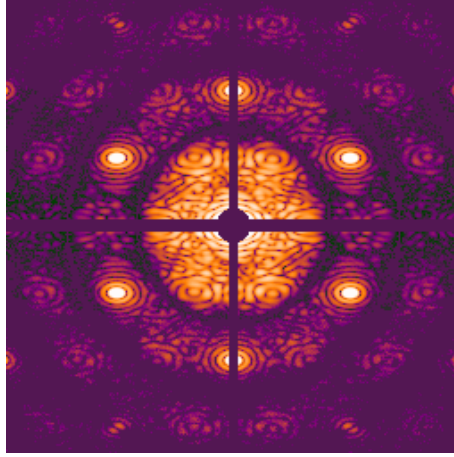
Figure 6: Reconstructed spherical sample with beamstop and statistical noise.

4.3 Ellipsoidal object with small beamstop

The real sample isn't always with a symmetrical shape. For this reason we want to try to reconstruct a colloidal object with an ellipsoidal shape and more not-symmetrical details, like in Fig. 7(a). The ellipse size is about 1380 x 2940 x 2530 nm. Beamstop region and statistical noise are also taken into account in this simulation.



(a) A 3D image of the real object.



(b) Simulated diffractive pattern.

Figure 7: Simulated scattering of the ellipsoidal sample.

The simulated pattern (see Fig. 7(b)) is obtained with the same wavelength $\lambda = 1.57$ Å and detector-sample distance $d = 5000$ mm, but with different detector size $l = 23$ mm. The resolution turns to be about 68 nm.

As before, an estimate of object size can be found from fringes in the diffraction pattern. Searching an approximate object shape is the first step of the reconstruction. We start with a rectangular support and running cycles as following one:

```
SizRec: 255 255 255
SizSup: 46 98 74
Positiv: 1
```

```
FixFreeEvolve 5 127
hio 100 1 0.9 0
er 5 1 0.8 0
ShrinkWrap 1 12 0
FixFreeEvolve 5 127
hio 80 1 0.9 0
er 5 1 0.8 0
ShrinkWrap 1 2 0 1.5
```

```

hio    80 1 0.9 0
er     5 1 0.8 0

```

The fourth value of *Shrink-Wrap* is the gaussian σ parameter: this function smooths the reconstructed image intensity with a gaussian distribution. Here it's necessary in order to fill the possible holes in the support, created by the first *Shrink-Wrap*. This function is very useful because we can avoid manual adjustment and to fill black holes in the support.

In Fig. 8, on the left, the support outputs of each cycles are shown: the value of gaussian and cutting parameters are gradually decreased.

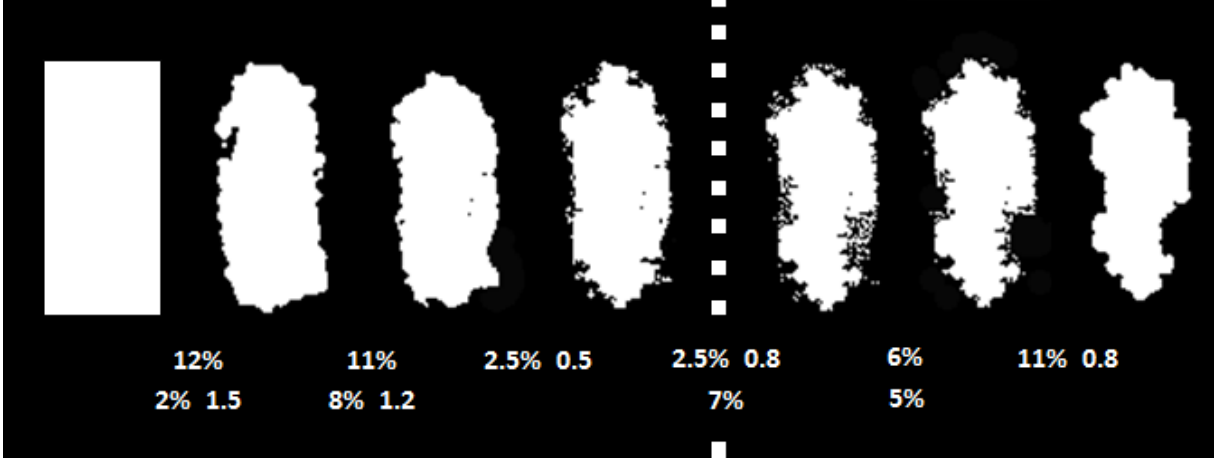


Figure 8: Support outputs for each reconstruction cycle (on the left the first step, on the right the second one). In the figure the cutting percentage and the *sigma* parameter (when it's used) are shown.

The second step is improving the support profile. It's not a trivial operation because for too low cutting values the result should be worse. Five runs of these functions

```

hio    100 1 0.95 0
er     5 1 0.8 0
ShrinkWrap 1 6 0
FixFreeEvolve 5 127
hio    50 1 0.95 0
er     5 1 0.8 0
ShrinkWrap 1 5 0
FixFreeEvolve 5 127
hio    50 1 0.95 0
er     5 1 0.8 0

```

are enough to clean the support from residual wrong regions. A last cycle with *ShrinkWrap 1 11 0 0.8* gets smooth our profile (see Fig. 8 on the right).

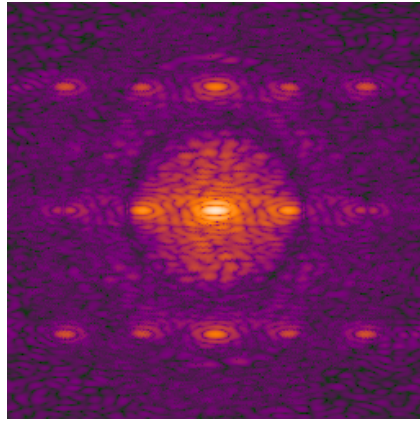
In the last step we can reconstruct the object. One hundred *hio* iterations are enough:

```

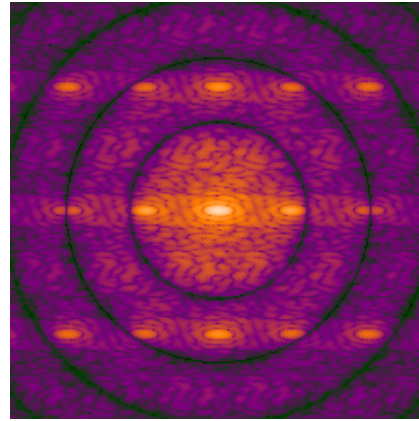
FixFreeEvolve 5 127
hio  80 1 0.9 0
er   5 1 0.8 0
FixFreeEvolve 5 127
hio  10 1 0.9 0
FixFreeEvolve 5 127
hio  10 1 0.9 0
er   5 1 0.8 0

```

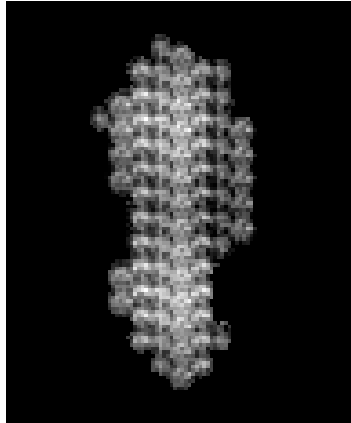
In order to obtain a nitid image, *FixFreeEvolve* is used more in the last iterations. The optional constraint of positivity is always imposed.



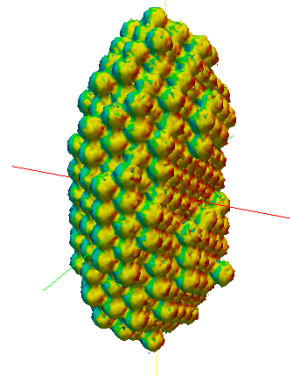
(a) The reconstructed reciprocal space.



(b) The ideal reciprocal space of the object.



(c) A slice of the reconstructed sample.



(d) 3D view of the reconstructed object.

Figure 9: Reconstructed ellipsoidal sample.

In Fig. 9 the reconstructed scattering amplitude is compared with the ideal reciprocal space of the sample: the missing center region has a good similarity with the actual case.

4.4 Ellipsoidal object with bigger beamstop and loose support

The experimental data has usually a bigger beamstop. We can try again to reconstruct the ellipsoidal sample with more information lack in the center, as in Fig. 10(a). With tight support it can be easily reconstructed. But usually tight support is unknown. Therefore we use bigger shape as initial support, like an estimate of the sample profile (Fig. 10(b)).

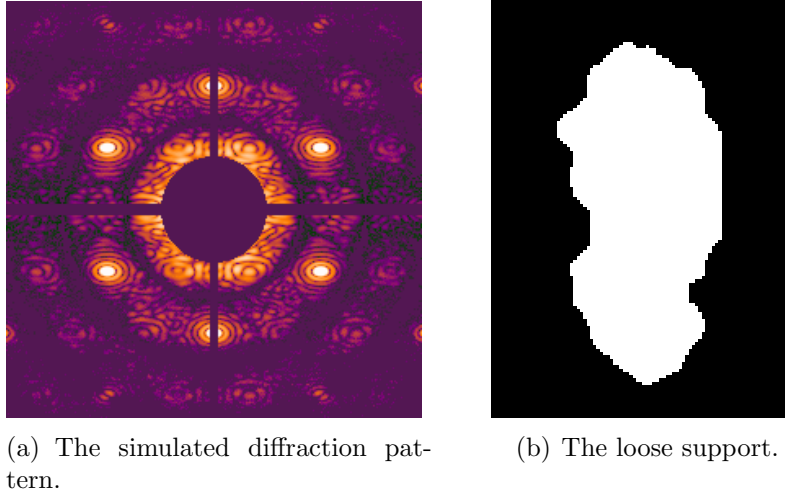


Figure 10: The initial data of the ellipsoidal sample with bigger beamstop.

As we have seen, the reconstruction is closely connected with the support shape. In this case the initial profile is not so good for a directly reconstruction. We have to change it through many cycles.

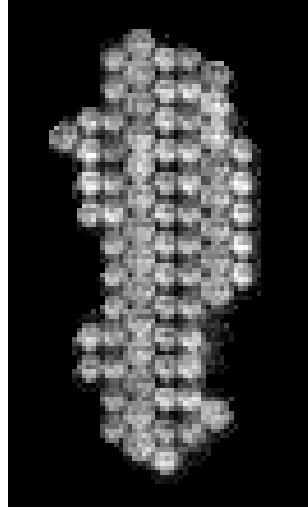
The basic idea is to cut gradually the wrong regions of the support: at the beginning they are one with the reconstructed image and it's difficult to distinguish them. We used a lot of times the usual reconstruction cycle with cutting and gaussian values smaller and smaller, as following:

Positiv 1

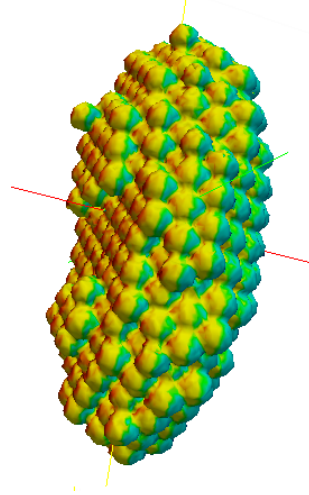
```
[...]  
FixFreeEvolve 50 127  
hio 100 1 0.8 0  
er 5 1 0.8 0  
ShrinkWrap 1 9 0 0.7  
FixFreeEvolve 50 127  
hio 90 1 0.8 0  
er 5 1 0.8 0  
ShrinkWrap 1 7 0 0.6  
FixFreeEvolve 40 127  
hio 80 1 0.8 0
```

```
er 5 1 0.8 0
ShrinkWrap 1 5 0 0.5
[...]
```

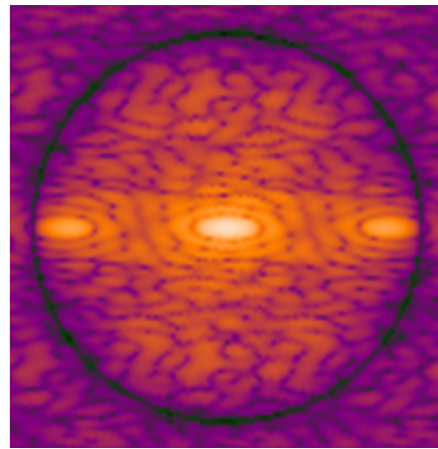
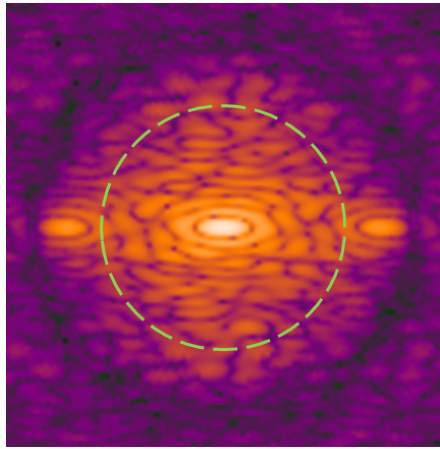
When we obtain a good support, the final reconstruction step is as before, in Par. 4.3. The result is shown in Fig. 11(a) and 11(b). Even with a bigger beamstop and loose support, it's possible achieve a good reconstruction of the sample. We can see the



(a) A slice through the reconstructed sample.



(b) The 3d view of the reconstructed object.



(c) A magnification of the reconstructed (on the left) and ideal (on the right) reciprocal space. In dashed green circle the beamstop region.

Figure 11: Reconstructed ellipsoidal sample.

reconstructed reciprocal space in the beamstop region (underlined by the dashed green circle) that is similar to the ideal one (Fig. 11(c)).

5 Conclusion

The CXDI is a good technique to explore the inner structure. As this report shows, it's possible to reconstruct the electron density distribution of a colloidal sample. Scattering pattern with 3 or 4 missing fringes can still be reconstructed.

The future work should be to apply this reconstructing method for measured data.

6 Acknowledgments

First of all, I would like to thank to my supervisor Ivan Vartanyants and to Summer Student program which made my work at Desy possible.

Special thanks to my adviser Oleksandr Yefanov, who patiently taught me my work and helped me during all these two months: I appreciated his advisers, corrections and his patience.

References

- [1] Jens Als-Nielsen and Des McMorrow. *Elements of Modern X-ray Physics*, Wiley, 2011
- [2] J. R. Fienup. Phase retrieval algorithms: a comparison. *Applied Optics*, 1982. Vol. 21, N. 15, 2758-2769